Journal of Information Engineering and Applications
ISSN 2224-5782 (print) ISSN 2225-0506 (online)
Vol.11, No.2, 2021

COMPARATIVE STUDY OF THERMAL CHARACTERISTICS OF METALLIC AND NONMETALLIC WATER-BASED NANOFLUIDS IN A SQUARE CAVITY

[1]EMMANUEL O. SANGOTAYO, AND [2]OLUKUNLE E. ITABIYI *
[1,2]Department of Mechanical Engineering, Ladoke Akintola University of Technology,
P.M.B. 4000, Ogbomoso, Nigeria.
[1]eosangotayo@lautech.edu.ng and [2]oeitabiyi@lauech.edu.ng*
*Corresponding author: oeitabiyi@lauech.edu.ng.

Abstract:
Heat transfer fluids are a dynamic factor that affects the costs and size of heat exchangers. However, low thermal properties of accessible coolants like water and oils place a setback on the growth of heat transfer to attain high-performance cooling. The paper presents a numerical analysis of a comparative study on thermal characteristics of Al_2O_3, CuO, AlN, and SiC water-based nanofluids in a square cavity. The cavity is surrounded by a hot moving horizontal plate, an adiabatic vertical wall on the right, and the left vertical and lower horizontal sides by cold isothermal walls. The governing equations were solved using finite approximation techniques to assess the thermal characteristics of the four different nanofluids in the enclosure with varying sizes of nanoparticles in the range of $1\% \leq \varphi \leq 10\%$. The results reveal that CuO has a different pattern of heat characteristics compared to other nanofluids. CuO has the highest Nusselt number of 58.4715, and Al_2O_3 has the least value of 58.4634 at a 10 % volume fraction. Nanoparticle size has a substantial influence on the thermal attributes of the four nanofluids. This work indicates that different nanofluids have satisfactory thermal characteristics than based fluid water, which determines its applications.
Keywords ***Cavity, Nanofluids, Natural convection, Heat transfer enhancement***
DOI: 10.7176/JIEA/11-2-08
Publication date: September 30th 2021

I. INTRODUCTION

Suspensions of solid sub-micron- and nanometer-sized particles in different fluids are called nanofluids, were considered for usage as an enhancement of heat transfer fluids for practically two decades. Though, as a result of the wide variety and the complicated nature of the nanofluid systems, no agreement has been attained on the magnitude of possibilities of benefits of using nanofluids for heat transfer applications (Wen, 2008). Numerous sizes of assessments were devoted to the characterization of different thermo-physical properties of nanofluids, such as thermal conductivity, viscosity, and clusters of nanoparticles (Wang and Mujumdar, 2007 & Sangotayo and Hunge, 2020).

Recent analyses reveal that nanofluids have numerous possibilities of applications in electronics cooling (Ijam and Saidur, 2012), refrigerators, nuclear reactor cooling, automobile radiators (Delavar & Hashemabadi, 2014), solar collectors (Goudarzi, 2014), plate heat exchangers (Tiwari. 2013), micro-pin-fin heat exchangers (Mohammadian, and Zhang, 2014), and mini channel heat sink (Ho and Chen, 2013). Kang et al.(2006) proved that using silver nanoparticles in distilled water inside the grooved heat pipe increases its thermal performance. The influence of nanofluids knowledge is estimated to be relevant, considering that the heat transfer performance of heat exchangers or chilling processes is essential in many industries (Murshed, 2008). Nnanna et al. (2009) produced a nanofluid heat exchanger for electronic cooling devices and showed how the system's effectiveness enriched concerning conventional apparatus. A numerical examination on fully advanced laminar mixed convection of nanofluids containing Al_2O_3 and water in a horizontal bowed duct was presented (Akbarinia and Behzadmehr, 2007). The result revealed that the volume fraction of nanoparticles does not have a direct effect on the axial velocity. A numerical examination of the cooling effectiveness of a microchannel heat sink with nanofluids was presented (Jang and Choi, 2006). Results showed that the thermal opposition and the heat variance of nanofluids reduced between the heated microchannel wall and the coolant.

Bianco et al.(2009) presented a simulation of the hydrodynamic and thermal behaviors of water–Al_2O_3 nanofluids flowing inside a uniformly heated pipe. Results showed that the accumulation of nanoparticles yielded a substantial enhancement in the heat transfer behaviour for the base liquid. Sangotayo and Hunge presented a numerical assessment of the impact of various nanoparticle concentrations on thermophysical characteristics and the convective heat transmission in a CuO nano-fluid-filled square enclosure. The result showed that nanoparticle sizes have a significant effect on heat distribution (Sangotayo and Hunge, 2020).

There were several models used for the estimating of the properties of nanofluids by several researchers; however, fewer studies were devoted to the effect of the nanoparticle size on thermal characteristics in different nanofluids. This paper presents a numerical examination of a comparative study on heat transfer behaviour and

thermal attributes of metallic and nonmetallic nanofluids such as Aluminum Oxide, Al_2O_3, Copper Oxide, CuO, Aluminum Nitride, AlN, and Silicon Carbide, SiC water-based nanofluids in a square cavity.

2.0 MATERIALS AND METHOD

This work presents a comparative numerical study on heat characteristics and thermal properties of four different metallic and nonmetallic nanoparticles such Al_2O_3, CuO, AlN, and SiC water-based nanofluids were used as coolants in a square cavity.

The Physical and the Mathematical Models

A continuously moving horizontal plate is evolving from an aperture at a velocity U_w and temperature T_w into four different still fluids, coolants as presented in Figure 1.0. The plate makes the upper wall of the cavity and is surrounded by an adiabatic vertical wall on the right, a fixed isothermal vertical wall adjacent to the extrusion die surface on the left and a fixed horizontal isothermal fence on the lower part, and The temperature T_w of the upper horizontal wall is higher than that of the lower horizontal wall (i.e., $T_w > T_\infty$) hence natural convective motion arose in the cavity. The flow is assumed steady, incompressible, laminar, and two-dimensional, and the fluid Newtonian. The internal heat generation and the heat transfer by radiation are assumed insignificant. The extrusion die wall is stationary and impermeable for which the non-slip boundary conditions are applied.

The flow governing equations at every point of the continuum consist of the expressions for the conservation of mass and momentum. These equations form a two-dimensional rectangular domain are (Ozisik, 1985):

Continuity equation:

$$\frac{\partial u}{\partial x} + \frac{\partial v}{\partial y} = 0 \qquad (1)$$

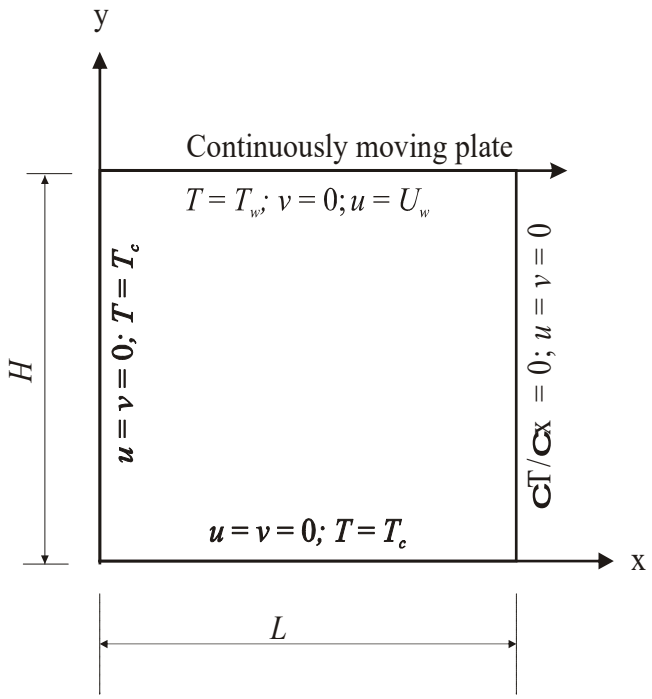

Figure 1: Schematic illustration of the physical model with the boundary constraints and the coordinate axes.

The Navier-Stokes equations in the *x*- and *y*-directions:

$$u\frac{\partial u}{\partial x}+v\frac{\partial u}{\partial y}=-\frac{1}{\rho_{nf}}\frac{\partial p}{\partial x}+\frac{\mu_{nf}}{\rho_{nf}}\left(\frac{\partial^2 u}{\partial x^2}+\frac{\partial^2 u}{\partial y^2}\right) \quad (2)$$

$$u\frac{\partial v}{\partial x}+v\frac{\partial v}{\partial y}=-\frac{1}{\rho_{nf}}\frac{\partial p}{\partial y}+\frac{\mu_{nf}}{\rho_{nf}}\left(\frac{\partial^2 v}{\partial x^2}+\frac{\partial^2 v}{\partial y^2}\right)+\frac{(\rho\beta)_{nf}}{\rho_{nf}}g(T-T_c) \quad (3)$$

where $\frac{(\rho\beta)_{nf}}{\rho_{nf}}g(T-T_c)$ is the force per unit volume in the *y*-direction.

The thermal energy transport equation

$$u\frac{\partial T}{\partial x}+v\frac{\partial T}{\partial y}=\alpha_{nf}\left(\frac{\partial^2 T}{\partial x^2}+\frac{\partial^2 T}{\partial y^2}\right) \quad (4)$$

where the density (ρ_{nf}), heat capacity$\left(C_p\right)_{nf}$, thermal expansion coefficient$(\beta)_{nf}$, and thermal diffusivity(α_{nf}) of the nanofluid are, (Kalbasi and Saeedi, 2012)

$$\rho_{nf}=(1-\varphi)\rho_f+\varphi\rho_s \quad (5)$$

$$\left(\rho C_p\right)_{nf}=(1-\varphi)\left(\rho C_p\right)_f+\varphi\left(\rho C_p\right)_s \quad (6)$$

$$(\rho\beta)_{nf}=(1-\varphi)(\rho\beta)_f+\varphi(\rho\beta)_s \quad (7)$$

$$\alpha_{nf}=\frac{k_{nf}}{\left(\rho C_p\right)_{nf}} \quad (8)$$

The Brinkman model is employed to estimate the dynamic viscosity of the nanofluids (Kalteh, 2001)

$$\mu_{eff}=\frac{\mu_f}{(1-\varphi)^{2.5}} \quad (9)$$

The effective thermal conductivity (k_{nf}) of the nanofluid with spherical nanoparticles is determined as (Kalbasi and Saeedi, 2012)

$$\frac{k_{nf}}{k_f}=\frac{k_s+2k_f-2\varphi(k_f-k_s)}{k_f+2K_s+\varphi\left(k_f-k_s\right)} \quad (10)$$

B. Method of Analysis and the Solution Techniques

The Navier-Stokes equations are a class of partial differential equations that could be classified as elliptic, parabolic, or hyperbolic depending on the problem under consideration. These equations can be solved by using either the vorticity-stream function approach or in their primitive-variable form. In this work, the vorticity-stream function approach is utilized, and so equations (2) and (3) are reduced to vorticity transport equation by eliminating the pressure gradient terms between the two, using the continuity equation (1), and the expression for the scalar value of the vorticity, ω, in the two-dimensional Cartesian coordinate system defined as

$$\omega=\frac{\partial v}{\partial x}-\frac{\partial u}{\partial y}. \quad (11)$$

The dimensional vorticity transport is the resulting expression, equation (12)

$$u\frac{\partial\omega}{\partial x}+v\frac{\partial\omega}{\partial y}=-\beta g\frac{\partial T}{\partial x}+\upsilon\left(\frac{\partial^2\omega}{\partial x^2}+\frac{\partial^2\omega}{\partial y^2}\right) \quad (12)$$

The derivatives of the stream function, ψ are the velocity components in two-dimensional Cartesian coordinate's Eqn (13)

$$u = \frac{\partial \psi}{\partial y}, \quad v = -\frac{\partial \psi}{\partial x} \tag{13}$$

which on substitution in equation (11) gives the Poisson equation for the stream function

$$\omega = -\left(\frac{\partial^2 \psi}{\partial x^2} + \frac{\partial^2 \psi}{\partial y^2} \right) \tag{14}$$

The derived transport equation, energy equation, and the prescribed boundary conditions were transformed in the non-dimensional form for a wide range of physical situations using L, (T_w - T_∞), U_W , $U_W L$ and U_W / L respectively for length, temperature, velocity, stream function, and vorticity (Chung,2002)

$$X = \frac{x}{L}, \quad Y = \frac{y}{L}, \quad U = \frac{u}{U_w}, \quad V = \frac{v}{U_w},$$

$$\theta = \frac{(T - T_\infty)}{(T_w - T_\infty)}, \quad \Psi = \frac{\psi}{U_w L}, \quad \Omega = \frac{\omega}{U_w / L},$$

The normalized form of the X- and Y-velocity components, stream function, vorticity, and energy transport equations are:

$$u = \frac{\partial \varphi}{\partial Y}, \quad V = -\frac{\partial \varphi}{\partial X} \tag{15}$$

$$\omega = -\frac{\partial^2 \varphi}{\partial X^2} - \frac{\partial^2 \varphi}{\partial Y^2} \tag{16}$$

$$u \frac{\partial \omega}{\partial X} - V \frac{\partial \omega}{\partial Y} = B\, Ra\, Pr \frac{\partial \theta}{\partial X} + A \left(\frac{\partial^2 \omega}{\partial X^2} + \frac{\partial^2 \omega}{\partial Y^2} \right) \tag{17}$$

where

$$A = {\mu_{nf}}/{(\rho_{nf} \alpha_{nf})}, \quad B = {(\rho\beta)_{nf}}/{\rho_{nf} \cdot \beta_f}, \quad Pr = {V_f}/{\alpha_f}, \quad Pr_{nf} = {V_{nf}}/{\alpha_{nf}}$$

$$u \frac{\partial \theta}{\partial X} + V \frac{\partial \theta}{\partial Y} = C \left(\frac{\partial^2 \theta}{\partial X^2} + \frac{\partial^2 \theta}{\partial Y^2} \right) \tag{18}$$

where

$$C = {\alpha_{nf}}/{\alpha_f}, \quad B = \frac{\rho_{nf} \beta_{nf}}{\rho_{nf} \beta_f} = {\beta_{nf}}/{\beta_f}.$$

In the above equations, k, thermal conductivity, μ, dynamic viscosity, Cp, specific heat capacity, *Re* Reynolds number, and *Gr,* Grashof number. The boundary conditions in the non-dimensional form are:

$$\Omega \neq 0; \Psi \neq 0; V = 0; U = \theta = 1 \text{ at } Y = 1; 0 \leq X \leq 1;$$

$$\Omega \neq 0; \Psi = U = V = \theta = 0 \text{ at } Y = 0; 0 \leq X \leq 1;$$

$$\Omega \neq 0; \Psi = U = V = \theta = 0 \text{ at } X = 0; 0 \leq Y \leq 1;$$

$$\Omega \neq 0; \Psi = \frac{\partial U}{\partial X} = \frac{\partial V}{\partial X} = \frac{\partial \theta}{\partial X} = 0 \text{ at } X = 1; 0 \leq Y \leq 1. \tag{16}$$

The vorticity and energy transport equations (17) and (18) are non-linear. One of the most fruitful methods for the resolution of equations (15) – (18) is the finite difference technique. The relaxation approach was adopted in solving the resulting simultaneously linear equations.

The temperature gradient that would result from the heat exchange process between the fluid and the wall is related to the local Nusselt number, Nu_x, through the following expression:

$$Nu_x = \frac{h_x x}{k} = -\left(\frac{\partial \theta}{\partial Y}\right)_{Y=1} \quad (17)$$

The average Nusselt number is calculated using the integration of the local Nusselt number over the entire length of the heated wall:

$$\overline{Nu} = \frac{\dot{Q}_{conv}}{\dot{Q}_{cond}} = -\int_0^1 \left.\frac{\partial \theta}{\partial Y}\right|_{Y=0 \, or \, 1} dX \quad (18)$$

The steady flow state was calculated by monitoring the convergence of the temperature and vortex field, using the following criterion:

$$\frac{\sum_{i=2}^{N}\sum_{j=2}^{M}\left|\phi_{ij}^{n+1} - \phi_{ij}^{n}\right|}{\sum_{i=2}^{N}\sum_{j=2}^{M}\left|\phi_{ij}^{n+1}\right|} < \delta \quad (19)$$

The parameter ϕ stands for Ψ, θ, or Ω and n represents the number of iterations before the convergence of the results. The value of δ used in different works of literature varies between 10^{-3} and 10^{-8} [19].

3.0 DISCUSSION OF RESULTS

The influence of the convergence standard on the numerical results was studied by calculating the average Nusselt number at various values of convergence parameter δ between 10^{-1} and 10^{-8}. The results are presented in Figure 2. It shows that an amount of $\delta = 10^{-4}$ was sufficient for convergence. The results of the grid independence tests give that a 41 by 41 grid system is adequate for excellent numerical stability, field resolution, and accurate results, as reported in a similar work carried out by Waheed [20].

The code of this work was validated by using the accuracy of the present simulation, and It is done by determining the Nusselt number for a convective flow of a similar problem was calculated as presented in Table 1.0. It is shown from Table 1.0 that there is good agreement with the computed Nusset number with about 2% differences.

Figure 3 presents the non-dimensional temperature profile for CuO, Al_2O_3, SiC, and AlN nanoparticle, at mid-plane, y = 0.5 along x coordinate. The chart shows that temperature distribution sharply increases along x from 0.0 - 0.1 enhances temperature gradient, then it reduces. CuO has the lowest, and Al_2O_3 has the highest temperature distribution along the x coordinate.

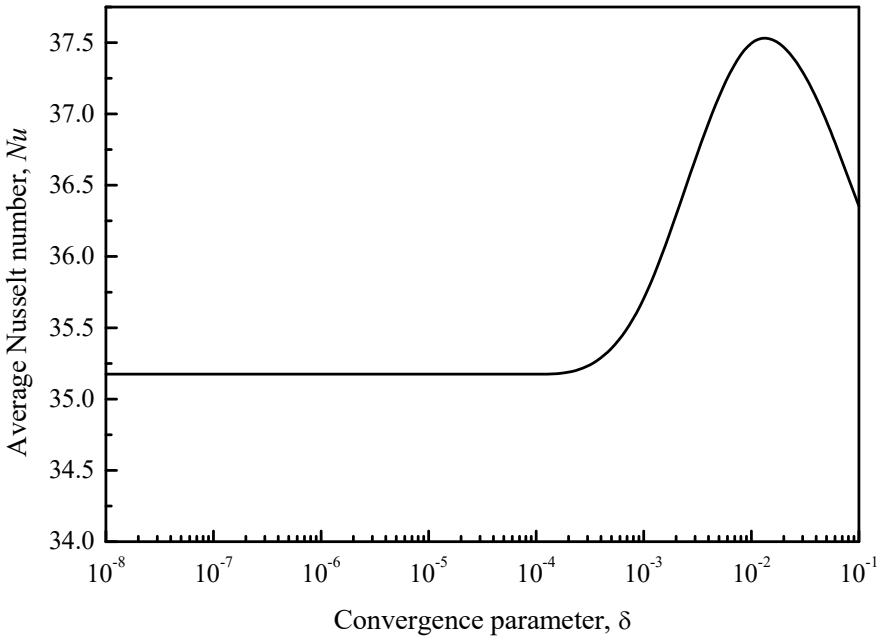

Figure 2: Plot of average Nusselt number, *Nu* versus the convergence parameter, δ

Table 1.0 Code Validation Results

Prandtl number, *Pr*	Rayleigh number, *Ra*	Nusselt number, Nu	Work
Pr = 0.7	*Ra* = 1000	*Nu* = 1.1210	Present
Pr = 0.7	*Ra* = 1000	*Nu* = 1.132	Waheed (2009)
Pr = 0.7	*Ra* = 10^5	*Nu* = 4.620.	Waheed (2009)
Pr = 0.7	*Ra* = 10^5	*Nu* = 4.7438	Present

Figure 4 presents the effect of varying nanoparticle sizes in the range of 0 % and 10 % on the Nusselt number. CuO has a different heat distribution pattern compares with Al_2O_3, SiC, and AlN. Heat distribution patterns in Al_2O_3, SiC, and AlN are similar. The convective heat transfer is slightly increasing and conductive heat transfer is slightly reducing in CuO nanofluid estimated as 0.002% as the nanoparticle sizes increase from 0 % to 10 % while in Al_2O_3, SiC and AlN, the convective heat transfer is growing rapidly and conductive heat transfer is reducing rapidly estimated as 0.02%. CuO has the highest Nusset number of 58.4715, SiC has 58.4636, AlN has 58.4641 and Al_2O_3 has the least value of 58.4634 at a 10 % nanoparticle concentration.

The effect of nanoparticle sizes on the density of different nanofluids is presented in Figure 5. Figure 5 displays that the mass of the nanofluid increases as the particle size increases. It shows that the thickness of nanofluid is directly proportional to its strength. CuO has the highest density of 1497 kg/m^3, Al_2O_3 has 1266 kg/m^3, AlN has 1223 kg/m^{3}and SiC has the least value of 1207 kg/m^3 at 10 % nanoparticle concentration.

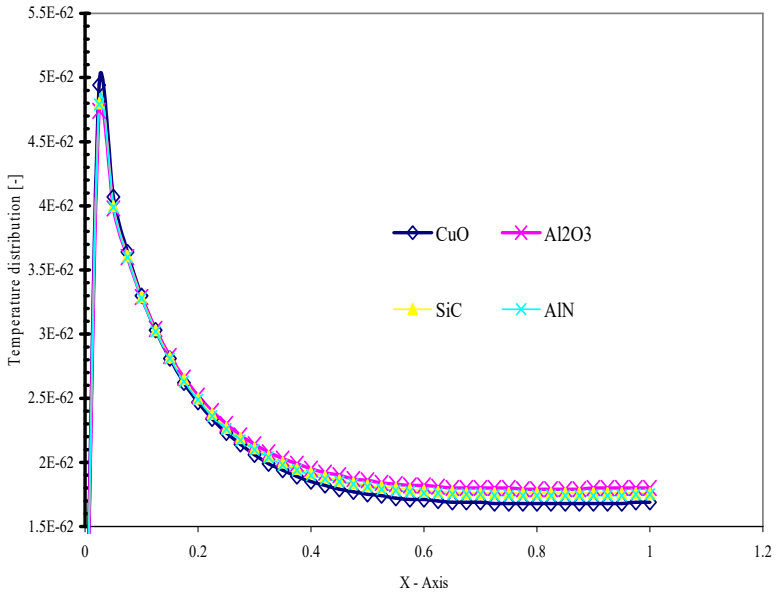

Figure 3 Temperature profiles for different nanofluids along X-axis at mid-plane, y = 0.5

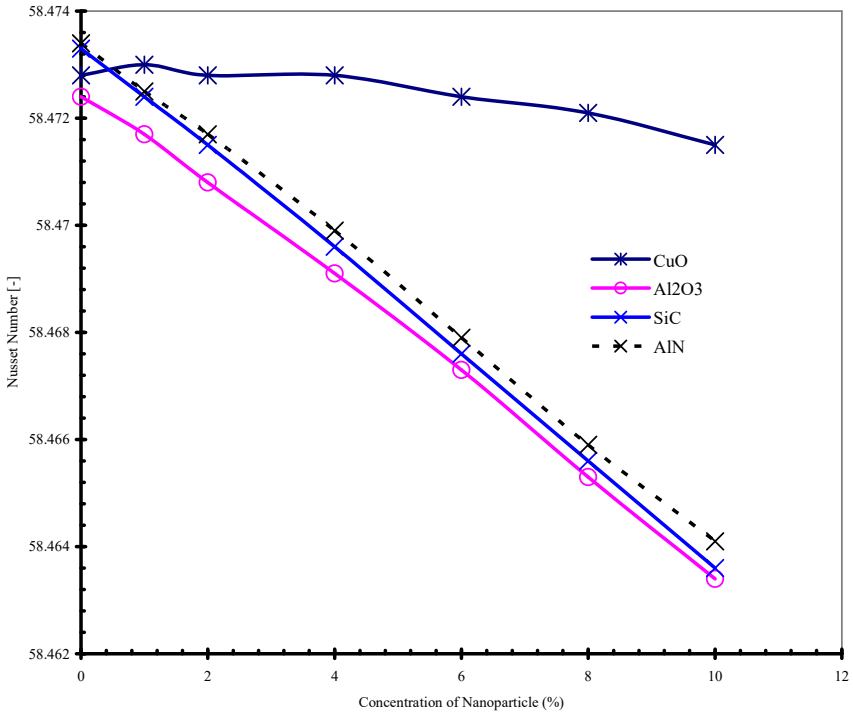

Figure 4.Graph of Nusselt number against the concentration of nanoparticles

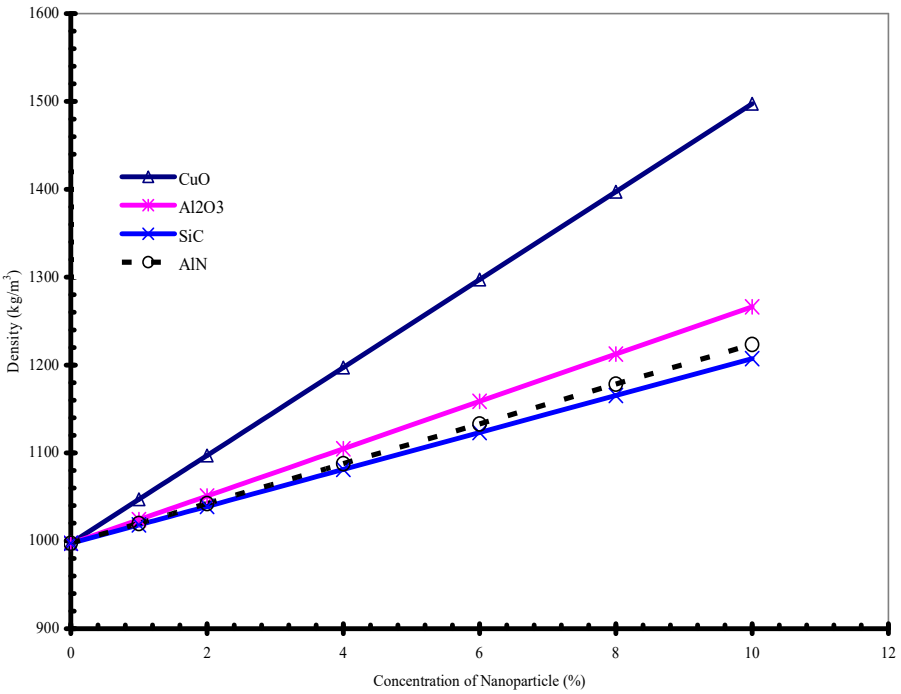

Figure 5 Graph of Density against Concentration of Nanofluids

Figure 6 displays the plot of the volumetric thermal coefficient for four different nanofluids versus the concentration of nanoparticles (0 % - 10 %). Figure 6 illustrates that there is a reduction in the volumetric thermal ratio of the nanofluids as the concentration of the nanoparticle is increased.

The influence concentration of nanoparticle sizes on thermal diffusivity for different nanofluids is displayed in Figure 7. Figure 7 shows that the thermal diffusivities of the nanofluids increase with an increase in the volume concentration of nanoparticles (0 % to 10 %). The effect of the strength of nanoparticle size on the Prandtl Number of the nanofluid is presented in Figure 8. Figure 8 displays that the momentum diffusivity of the fluid is increasing, and thermal diffusivity is reducing as the volume fraction of nanoparticle increase from 0 % to 10 %.

Figure 9 presents the influence of the concentration of nanoparticle size on the thermal conductivity of the nanofluids. It displays that nanofluid thermal conductivity increases with an increase in the level of nanoparticle sizes in different nanofluids. Al_2O_3 has the highest thermal conductivity of 0.399067 W/mK, CuO has 0.393711 W/mK, SiC has 0.388974 W/mK, and AlN has the least value of 0.38837 W/mK at a 10 % concentration of nanoparticle. It is supported by many authors (Wen et al. 2009, Wang and Mujumdar, 2007 & Sangotayo and Hunge, 2020).)

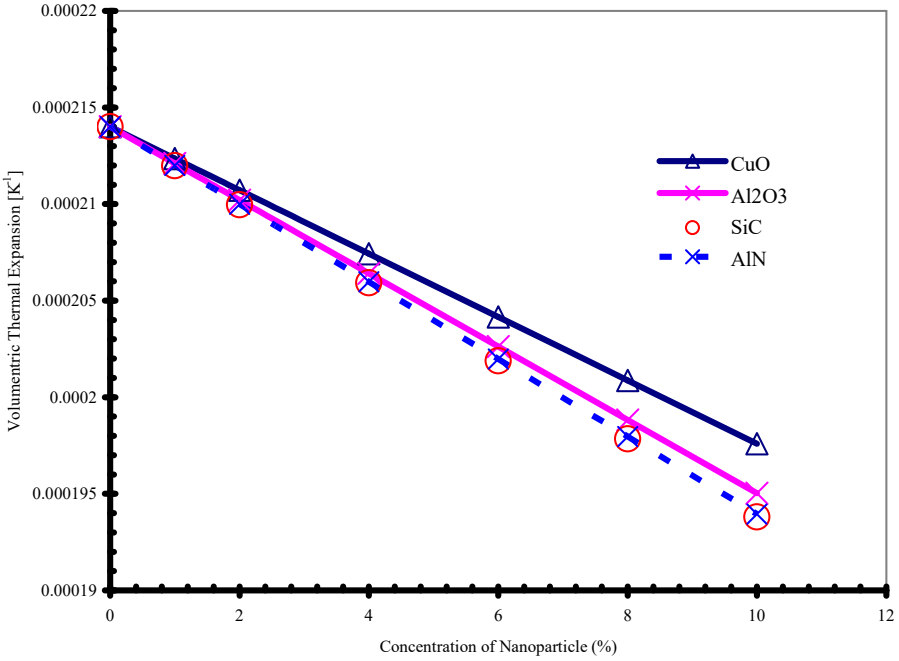

Figure 6 Graph of Volumetric thermal coefficient against volumetric concentration.

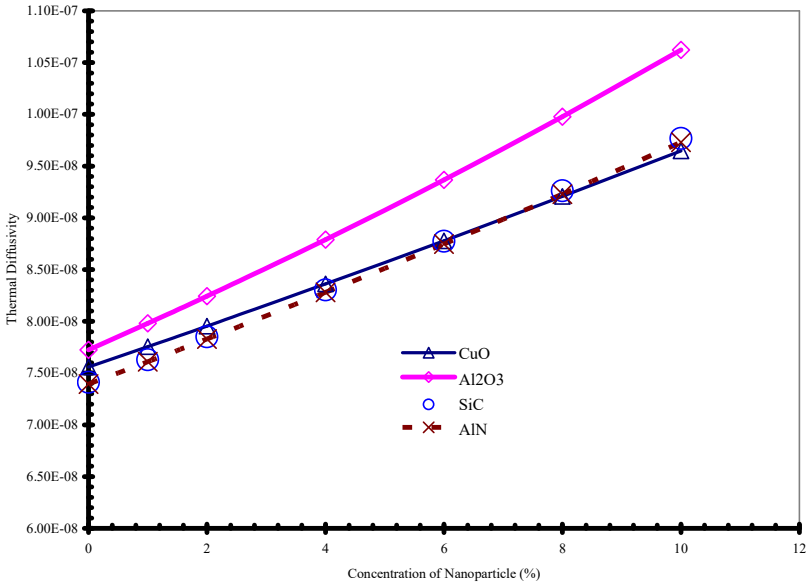

Figure 7 Diagram of Thermal Diffusivity against Concentration of Nanoparticle

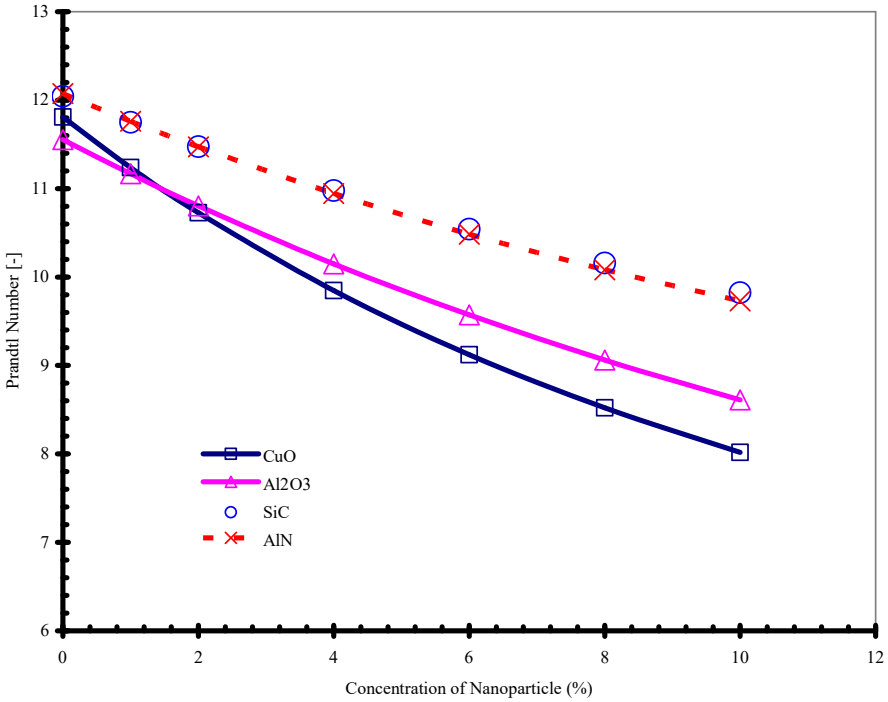

Figure 8 Plot of Prandtl Number [-] vs Concentration of Nanoparticle (%)

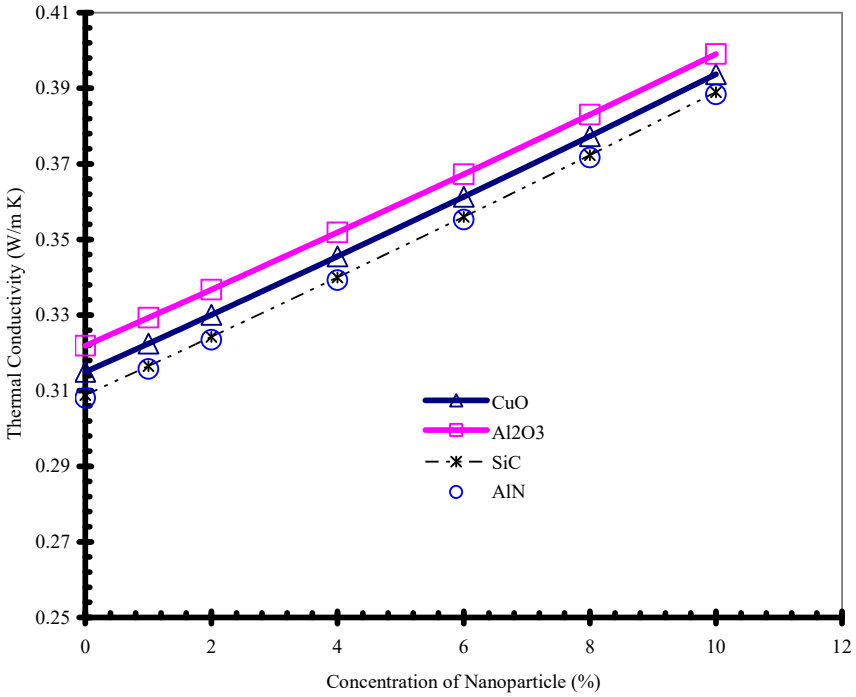

Figure 9 Graph of Thermal Conductivity against Concentration of Nanoparticle

Figure 10 displays the effect of the concentration of nanoparticle size on the specific heat capacity for different nanofluids. It displays that the specific heat capacities of the nanofluids are reducing as the nanoparticle

size increase from 0 % to 10 %. SiC has the highest specific heat capacity of 3836.1 AlN has 3835.1 W/mK, CuO has 3816.2 W/mK and Al_2O_3 has the least value of 3762.9 W/mK at 10 % nanoparticle size.

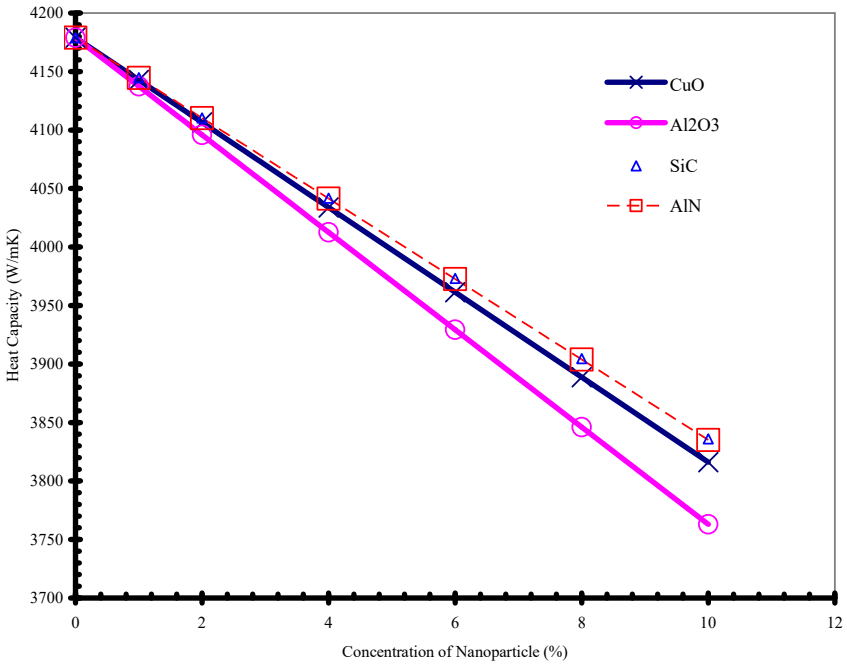

Figure 10 Graph of Specific Heat Capacity against Concentration of Nanoparticle

4.0 CONCLUSIONS

Heat transfer fluids are an essential factor that affects the dimensions and prices of heat exchangers. Numerical simulation of a comparative analysis on heat transfer behaviour and thermal features of metallic and nonmetallic nanofluids such as Aluminum Oxide, Al_2O_3, Copper Oxide, CuO, Aluminum Nitride, AlN, and Silicon Carbide, SiC water-based nanofluids in a square enclosure was carried out in this work. The results reveal that CuO has a different pattern of heat characteristics compared to Al_2O_3, AlN, and SiC water-based nanofluids, while Al_2O_3, AlN, and SiC have similar trends. Nanoparticle size has a significant impact on heat distribution and the thermal attributes in the four nanofluids; hence this work indicates that the suspended nanoparticles significantly change the thermal characteristics of the suspension which determines its applications

References

Akbarinia, A. and Behzadmehr, A., (2007) Numerical Study of Laminar Mixed Convection of a Nanofluid in Horizontal Curved Tubes, *Appl. Therm. Eng.*, vol. 27, pp. 1327–1337.

Bianco, V., Chiacchio, F., Manca, O., and Nardini, S., (2009) Numerical Investigation of Nanofluids Forced Convection in Circular Tubes, *Appl. Therm. Eng.*, vol. 29, pp. 3632–3642.

Chung, T. J. (2002). *Computational Fluid Dynamics*. Cambridge University Press, Cambridge.

Delavari, V. and Hashemabadi, S.H., (2014) CFD Simulation of Heat Transfer Enhancement of Al_2O_3/Water and Al_2O_3/Ethylene Glycol Nanofluids in a Car Radiator, *Appl. Therm. Eng.*, vol. 73, pp. 378–388.

Goudarzi, K., Shojaeizadeh, E., and Nejati, F., (2014) An Experimental Investigation on the Simultaneous Effect of CuO-H_2O Nanofluid and Receiver Helical Pipe on the Thermal Efficiency of a Cylindrical Solar Collector, *Appl. Therm. Eng.*, vol. 73, pp. 1234–1241.

Ho, C.J. and Chen, W.C., (2013) An Experimental Study on Thermal Performance of Al_2O_3/Water Nanofluid in a Minichannel Heat Sink, *Appl. Therm. Eng.*, vol. 50, pp. 516–522.

Ijam, A. and Saidur, R., (2012) Nanofluid as a Coolant for Electronic Devices, *Appl. Therm. Eng.*, vol. 32, pp. 76–82.

Jang, S.P. and Choi, S.U.S., (2006) Cooling Performance of a Microchannel Heat Sink with Nanofluids, *Appl.Therm. Eng.*, vol. 26, pp. 2457–2463.

Kalbasi, M., and Saeedi, A. (2012) "Numerical Investigation into the Convective Heat Transfer of CuO Nanofluids Flowing Through a Straight Tube with Uniform Heat Flux," Indian Journal of Science and Technology 5 (S3), pp. 2455-2458, Iran;

Kalteh, M., Abbassi, A., Saffar-Avval, M. and Harting, J. (2011) "Eulerian Two-Phase Numerical Simulation of Nanofluid Laminar Forced Convection in a Microchannel," International Journal of Heat and Fluid Flow 32, pp. 107-116,

Kang, S.W., Wei, W.C., Tsai, S.H., and Yang, S.Y., (2006) Experimental Investigation of Silver Nanofluid on Heat Pipe Thermal Performance, *Appl. Therm. Eng.*, vol. 26, pp. 2377–2382.

Mohammadian, S.K., and Zhang, Y., (2014) Analysis of Nanofluid Effects on Thermoelectric Cooling by micro-Pin- Fin heat Exchangers, *Appl. Therm. Eng.*, vol. 70, pp. 282–290.

Murshed, S.M.S., Leong, K.C., and Yang, C., (2008) Thermophysical and Electrokinetic Properties of Nanofluids— ACritical Review, *Appl. Therm. Eng.*, vol. 28, pp. 2109–2125.

Nnanna, A.G.A., Rutherford, W., Elomar, W., and Sankowski, B., (2009) Assessment of Thermoelectric Module with Nanofluid Heat Exchanger, *Appl. Therm. Eng.*, vol. 29, pp. 491–500.

Ozisik, M.N., (1985). *Heat Transfer, A Basic Approach*. International Textbook Company, Seraton, Pa.

Sangotayo Emmanuel O. and Hunge Oluwashina N., (2020) " Numerical Analysis of Nanoparticle Concentration Effect on Thermo-physical Properties of Nanofluid in a Square Cavity " , *International Journal of Mechanical and Production Engineering (IJMPE)*, Volume-8, Issue-2, pp. 18-23

Tiwari, A.K., Ghosh, P., and Sarkar, J. (2013) Heat Transfer, and Pressure Drop Characteristics of CeO_2/Water Nanofluid in Plate Heat Exchanger, *Appl. Therm. Eng.* vol. 57, pp. 24–32.

Waheed, M.A. (2009). "Mixed convective heat transfer in rectangular enclosures driven by a continuously moving horizontal plate". *International Journal of Heat and Mass Transfer*, 52, pp. 5055–5063

Wang XQ, Mujumdar A.S. (2007) Heat transfer characteristics of nanofluids: a review. Int J Therm Sci, 46(1):1-19.

Wen D.S, Lin G.P., Vafaei S, & Zhang K (2009,): Review of nanofluids for heat transfer applications. Particuology 7(2):141-150.